ELSEVIER

International Journal of Mass Spectrometry 176 (1998) 189–201

International Journal of Mass Spectrometry

Negative ionization processes of osmium for isotopic measurements

Kéiko Hattori[a,*], T. James S. Cole[a], Douglas P. Menagh[a,b]

[a]*Department of Geology, the University of Ottawa, Ottawa, K1N 6N5 Canada*
[b]*Department of Physics, Carleton University, Ottawa, K1S 5B6 Canada*

Received 8 December 1997; accepted 29 March 1998

Abstract

Negative ion mass spectrometry (N-TIMS) for many elements requires O_2 gas, thermal electrons, and hot filament temperatures. These requirements are partly in conflict. For example, O_2, essential for volatilization of refractory metals, has "poisoning" effects on electron emission. Hot filament temperatures enhance reactions, but greater thermal electron emission distorts the source ion optics. Our work suggests an ionization scheme where Os is oxidized to gaseous OsO_3, with this neutral molecule ionized to OsO_3^-, primarily by electron capture very close to the hot filament. Lesser, but significant, numbers of ions are formed by electron exchange with O^- away from the filament, which results in the commonly observed asymmetric peak shape. Repeated neutralization–ionization produces ions with low potential energies, which cause significant tailing of peaks on the high mass side. Low energy ions account for problems reported in N-TIMS by previous workers, including high background base lines, asymmetric peaks and poor reproducibility of isotopic ratio measurements. This interpretation is not in accord with the prevailing view that both positive and negative ionization, with a low energy spread, takes place on the filament surface. It is supported by observations previously reported, such as the widely recognized "memory effects" in N-TIMS. Declining ion intensities at higher filament temperatures, reported as puzzling maxima by previous workers, are also consistent with the proposed model. Excess electrons play a significant role in the source ion optics. (Int J Mass Spectrom 176 (1998) 189–201) © 1998 Elsevier Science B.V.

Keywords: Negative ionization; Isotope mass spectrometry; Thermal ionization; Osmium; N-TIMS

1. Introduction

Negative ion mass spectrometry (N-TIMS) is a standard technique for the isotopic ratio measurements of refractory elements, such as Os [1–3], Ir [3,4], W [5], Ru [6], and Pt [7], because these elements are difficult to ionize in conventional positive ion mass spectrometry (P-TIMS). Conversion from P-TIMS to N-TIMS can be easily achieved by reversing the polarity of the magnet and of the extraction plates in the source of mass spectrometers. This ease of the conversion has led to extending the application of N-TIMS to several other elements, including Cl, B, and O [8–11], for which P-TIMS is the usual technique. Advantages of N-TIMS include simpler sample preparation and higher efficiency of ionization, which reduces sample size requirements.

Both positive and negative ionization are com-

* Corresponding author. E-mail: khattori@uottawa.ca

PII S1387-3806(98)14021-6

monly considered to take place on the "filament surface" [10,12,13], with a small ion energy spread [14]. This led to use of the term *surface ionization mass spectrometry* synonymously with P-TIMS and N-TIMS [14,15]. Ionization is commonly expressed by the Langmuir-Saha equation for positive ions and by the revised form of the Langmuir-Saha equation for negative ions [1,8,10,12,13,16]:

$$\beta^+ = N_+/(N_0 + N_+)$$
$$= [1 + g_0/g_+ \exp[(\mathrm{IP} - \Phi)/kT]^{-1}$$
$$\beta^- = N_-/(N_0 + N_-)$$
$$= \{1 + g_0/g_- \exp[(\Phi - \mathrm{EA})/kt]\}T^{-1}$$

where N_0, N_+, and N_- are the numbers of neutral species, and positive and negative ions, respectively; β^+ and β^- are the ion yields for positive and negative thermal ions; g_0, g_+, and g_- are the partition functions of the neutral species and positive and negative ions; IP is the first ionization potential of the analyte; Φ is the electron work function of the filament material, EA is the electron affinity of the analyte; k is the Boltzmann constant and T is the temperature in Kelvin.

These equations, which were originally derived to explain the ionization of alkali metals [17], include the principal parameters for ionization, such as temperatures and work functions of the filament material, but were intended to describe the equilibrium state and not the dynamic process of ionization in the mass spectrometer. Therefore, the equations do not explain problems commonly observed during N-TIMS, such as different isotopic ratios at different filament temperatures [18], sloping peak tops (e.g. Fig. 3 of Creaser et al. [1]) and high and asymmetrical baselines [6,7]. Declining ion intensities at higher temperatures are another puzzling feature [1,2,6,16,19], because the Langmuire-Saha equations predict higher ion intensities at higher temperatures. The widely known "memory effects" of N-TIMS are also an unexpected feature for people familiar with P-TIMS. In this article, we describe the negative ionization process of Os and compare the fundamental differences of ionization between P-TIMS and N-TIMS.

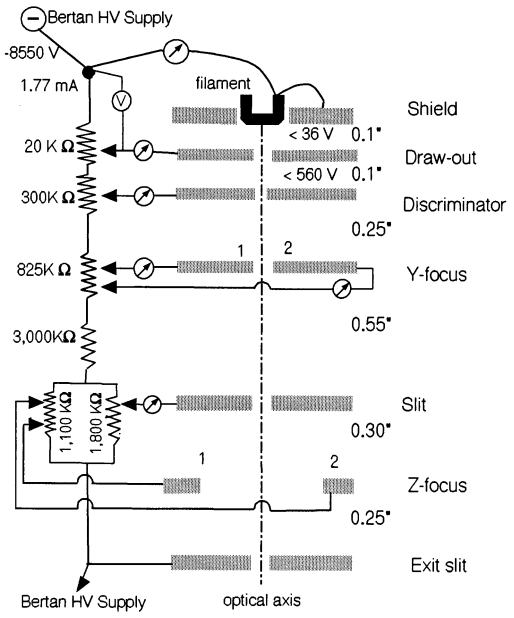

Fig. 1. Schematic configuration of the ion source. Digital microammeters, shown as an arrow in a circle, are placed to measure the electron currents. The ammeter connected to the filament and the negative high voltage supply provided the total electron emission. The ammeters connected to draw-out plates, discriminator plates, Y-focus plates, and slit plates provided the electron current through the corresponding plates. A voltmeter, shown as a V in a circle, is placed between the HV supply and each ion source plate. The diagram shows the placement of the voltmeter for the draw-out plate. The total accelerating voltage was 8.55 kV. The potentials of draw-out and discriminator plates can be changed up to 36 and 560 V, respectively.

The information is applicable to other elements and is useful for further development of N-TIMS and accurate isotopic ratio measurements with N-TIMS.

2. Instrumentation and osmium sample preparation

2.1. Mass spectrometer

This study used a modified 12-in. mass spectrometer made by NBS (currently National Institute of Standards and Technology, Washington DC) with a collector housing unit by Nuclide Corporation (currently Premier American Technologies Corporation, PA). The schematic configuration of the ion source is

Table 1
Specification of the mass spectrometer

Flight tube	12 in. radius, 68° deflection
Magnet coil	Cu rectangular tube, 54 turns each with total 0.06 Ω, with continuous flow of closed-loop chilled water inside the tube
O_2 supply	Stainless steel capillary tube (0.5 m) and a bellow (500 mL)
Ion accelerating voltage	Total <20 kV, normally 8.55 kV for Os by Bertan Model 210-20- R
Source exit slit	0.004 or 0.008 in.
Collector housing	Collector housing made by Nuclide Corp. (Premier American Technologies Corp., PA) with Faraday cup and multiplier
Collector slit	Width adjustable (≤0.04 in.), rotatable (360°)
Magnet supply	Custom-made three phase bridge rectifier power supply (<9 VDC, <150 A on a continuous basis with a peak current of ~900 A), with filter capacitor of 1.2 F
Magnet field control	Modified nuclide magnet field control unit and custom-made negative feed-back amplifier
Pulse integration	Vibrating capacitor electrometer[a] (model 401), Cary Instruments
Pulse amplifier	Custom-built nanosecond pulse amplifier and pulse height discriminator
Secondary electron multiplier	Nuclide SEM; 10 ns rise time and 10^5 gain with 10^9 Ω feedback resister
Ion current sensitivity	10^{-18} A
Ion current tail discrimination	<0.001 of a peak at 0.5 u above and below the peak centre for both negative and positive ions
Control system	Graphic user interface
Computer interface	HP IEEE 488 interface unit in a PC

[a] This was chosen because the capacitor is near ideal with its sapphire insulators and gold plated, inert gas filled.

shown in Fig. 1. The original source unit and flight tube were used because of the excellence of the design for ion focusing, but all electronic components were replaced (Table 1). The source had an O_2 supply system with a stainless steel capillary tube and a bellows (≤500 mL). The mass spectrometer is controlled and operated by a Windows-based program through IEEE 488 interfaces, including the power supply and data collection.

2.2. Magnet

To reduce the inductance of the magnet and its settling time constant, the magnet coils were rewound with rectangular Cu tube of low resistance (total 0.06 Ω), through which chilled water was circulated. The cool, constant temperature of water ensured a precise shape of the flight tube and the dimension between the source and collector slit, thus yielding stable ion currents at a given mass setting. In addition, this minimized a variation in the output of the Hall effect magnetic field sensor because of a temperature fluctuation.

The rewinding of the magnet was designed to attain a short stabilization time after a change in the magnetic field. The time constant τ for stabilization of current through the magnet coils is expressed by $\tau = L/R$, where L = inductance and R = resistance. Because the inductance L is proportional to N^2 and the resistance R is proportional to the turns of magnetic coils N, a shorter time constant τ and a faster magnetic field response time were obtained by fewer turns of coils. The magnetic field of the iron core began to saturate at 7500 G, corresponding to a magnet coil current of 150 A at 9 V.

A transient change in B induces eddy currents in the magnet core and some small, localized magnetic hysteresis loops in the pole faces, but these effects were taken care of by the magnetic control system.

The dc magnet power was supplied by a custom-made, bridge-rectified, three phase, 208 VAC power supply, which can deliver up to 150 A on a continuous basis, with a peak capability of ~900 A at 10 V. To maintain the magnetic flux below the saturation level, the operating current was below ~130 A. Compared with single phase rectification, three phase rectification greatly reduced ac ripple in the dc output. A filter capacitor of 1.2 F stored more than sufficient energy during the magnetic field stepping.

Table 2
Mass ratios of Os oxide in Os standard solution except for the Nier values [35]

Ref.	240/236	238/236	Uncertainty	237/236	Uncertainty	235/236	Uncertainty
Nier	3.09591	1.9934		1.2168		0.12379	
Yin[a]	3.09217	1.98956	0.00011	1.22066	0.00074	0.174408	0.000014
Hauri[b]	3.09217[c]	1.9896	0.0026	1.2207	0.0009	0.1736	0.0003
This work[d]							
1	3.09217[c]	1.9904	0.0038	1.2217	0.0026	0.1732	0.0007
2	2.09217[c]	1.9882	0.0017	1.2226	0.0011	0.1759	0.0003
3	3.09217[c]	1.9883	0.0018	1.2195	0.0012	0.1726	0.0003
4	3.09217[c]	1.9844	0.0032	1.2185	0.0018	0.1747	0.0005
5	3.09217[c]	1.9879	0.0002	1.2200	0.0014	0.1748	0.0002
Average	3.09217[c]	1.9878	0.0019	1.2204	0.0012	0.1743	0.001

Yin [21] and Hauri [24] presented nonoxide values; these are recalculated using the oxygen isotope abundance values of Nier [22] to provide the comparison.

[a] Average of 7 runs on page 56 of Yin [21].

[b] Average of 10 runs, p. 176 in Hauri [24].

[c] Normalized value.

[d] 1–5; this study: 1 s data collection time for each peak with delay time of 750 ms between peaks. Each run collected 100 measurements of masses ranging from 234 to 242 u.

2.3. Pulse counting and pulse integration

The collector slit was adjustable for both width and angle, to match the axis of the flight tube. The Faraday cup could be opened to allow ions to pass through the secondary electron multiplier (SEM) for either pulse counting or pulse integration. The performance of ion counting with the SEM was checked by its output shape of single pulses on an oscilloscope at low ion beam current ($\sim 10^{-16}$ A). The output pulses had about a 10-ns rise time. The SEM output pulses were fed into a custom made pulse amplifier suitable for the TTL logic circuit of frequency counter. A discriminator circuit eliminated noise pulses.

We chose the vibrating capacitor electrometer made by Cary Instruments, Monrovia, CA for pulse integration because of its excellent input capacitor. Using a 10^{11} Ω feedback resistor at the input and a Faraday cup collector, 10^{-14} A ion current yielded 1 mV output. Using a multiplier voltage of 2860 V (145 V per stage) and a 10^{9} Ω feedback resistor, SEM delivered 1 V output from an ion current of 10^{-14} A.

2.4. Mass spectrometer setup

The magnet position and ion source parameters were adjusted to produce a well-focused beam of positive Sr ions. Ions of mass M are related to magnetic field B and potential V by the equation $M = (e/m_u)*(r^2/2V)*B^2$, where r = radius and $e/m_u = 9.6485308 \times 10^{-7}$ C kg^{-1}. The values of r and V were not exactly known, and the mass spectrometer constant ($r^2/2V$) was obtained from B and M. A linear fit of B^2 versus M was obtained for all Sr isotopes, yielding the constant of 4.88002 ± 0.00001 (2 σ) u tesla^{-2}. This constant was used to obtain M from B, M = constant $*B^2$, for the operation of the mass spectrometer.

Well-resolved negative ion beams of many species were observed after adjustment of ion source parameters. The performance is further examined using an Os "shelf" standard, of which isotopic ratios have been determined at several institutions (Table 2). Os oxide isotope ratios were obtained from the least-square fit lines of peak intensities of various masses (y axis) and the intensity of mass 236 (x axis; Fig. 2) [20]. The uncertainties of the ratios were also calculated from both coordinates, following the method described by Moreno [20]. The ratios were normalized to 240/236 = 3.092172 using ^{192}Os/^{188}Os = 3.08261 by Yin [21] and O isotope abundance of Nier [22]. There is uncertainty of O isotope abundance [11,23], but the O correction for the conversion from

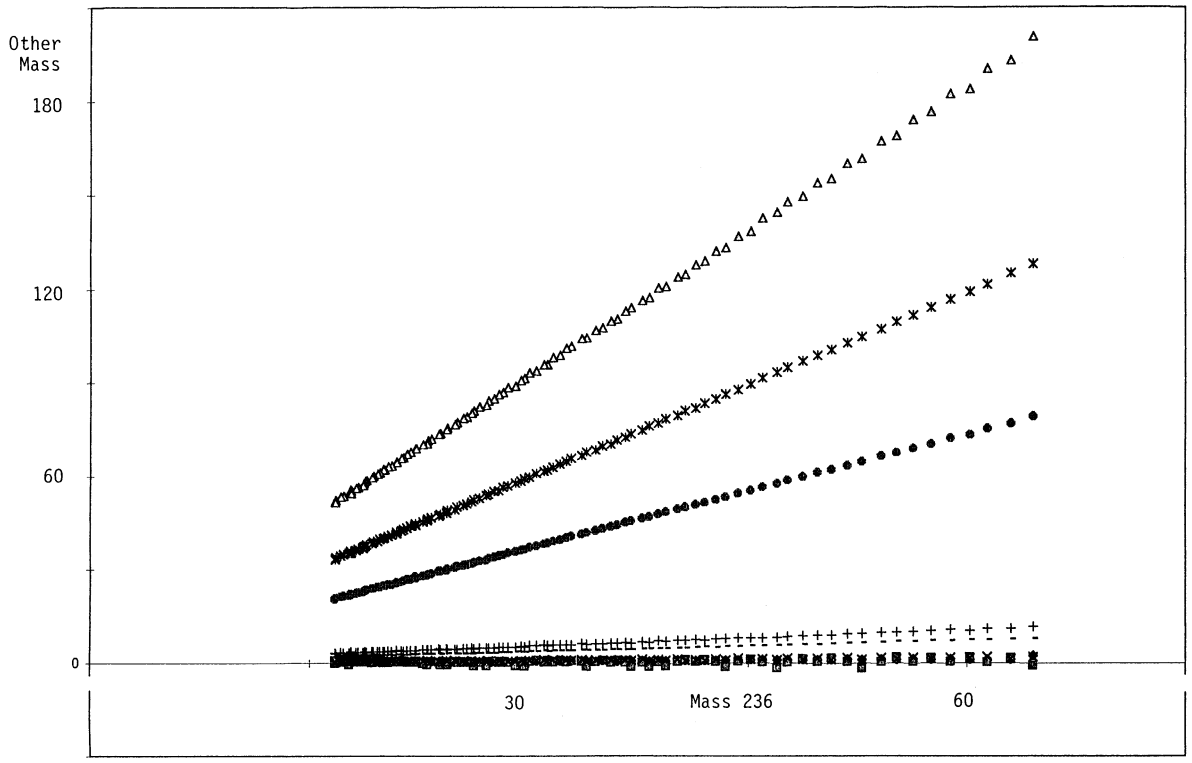

Fig. 2. Plot of peaks for calculation of peak ratios, following the method described by Moreno [20]. The peak intensities were collected using the Faraday cup with collection time of 1 second and delay time of 750 ms. Each point represents peak intensity in millivolts for the m/z 236 (x axis) and the other m/z values (240, 238, 237, 235, 234, and 232; y axis). Thus, the slope gives the mass ratios. The steepest slope formed by triangles is for m/z 240 in y axis. Gentler slopes correspond m/z 238, 237, 237, 235, and 234.

oxides to metal ratios is small and the use of different O isotope abundance has negligible effects on the calculation. Our results are similar to those reported by Yin [21] and Hauri [24] and the results obtained by the author using a 9-in. NBS mass spectrometer at the Woods Hole Oceanographic Institution (WHOI).

2.5. Osmium standard

A solution of Os chloride (0.5–1 ngOs) was placed on a Pt filament (5 N, 0.001-in.-thick, 0.020-in.-wide, Electronic Space Products International, Ashland, OR) and evaporated at ~0.8 A, before being reduced to Os metal under vacuum ($<10^{-6}$ Torr) at ~700°C for 4–5 h. The reduction of compounds to metal is a standard technique for isotopic analysis of platinum group metals [6,21,24]. Os compounds, such as $OsCl_3$ and $OsBr_3$, loaded on filaments decompose into shiny Os metal and halogens on heating in vacuum. The reduction before mass spectrometry is favorable, especially for small samples because it produces long-lasting steady peaks.

After the reduction, ~0.5 μL of saturated $Ba(NO_3)_2$ solution (Aldrich Chemical Co., Milwaukee, WI, 20275-4) was applied to cover the Os and evaporated at 0.8 A. All experiments were carried out using a single filament assembly using a standard fused glass bead of Associated Electrical Industries, Manchester (AEI-mount filament) and a standard NBS stainless steel bead (NBS-mount filament).

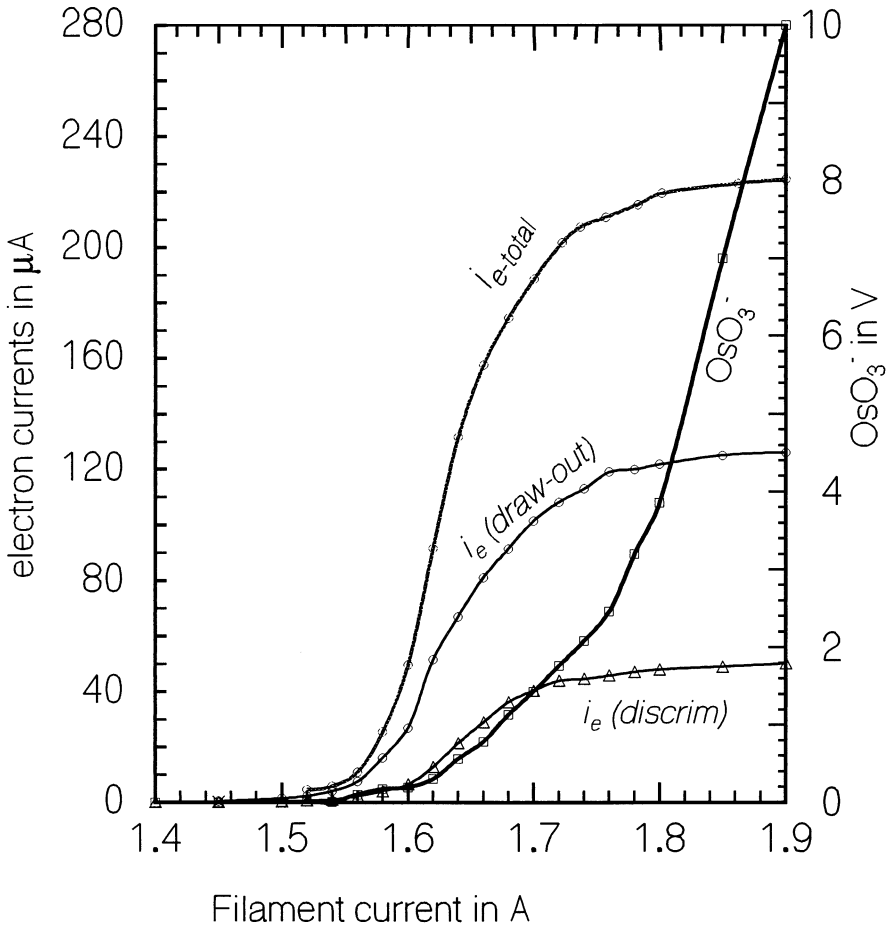

Fig. 3. The intensity of OsO_3^- ion in volts and thermal electron emission at different filament temperature. Output of 1 V corresponds to 10^{-14} A ion current. i_e-total = total electron emission, i_e (draw-out) = electron current on the draw-out plates at a potential of 26 V, i_e(discrim) = electron current on the discriminator plate at a potential of 196 V. Experimental condition: AEI-mounted Pt-filament, electron multiplier was set at 2860 V, P_{O_2} = 9.4 to 9.9 × 10^{-8} Torr. An AEI-mounted fused glass bead was a standard assembly for mass spectrometers made by Associated Electrical Industries, Manchester. The filament temperatures were determined using an optical pyrometer through silica-glass window.

3. Relationship between different parameters

3.1. Electron emission and the filament current

As expected, more thermal electrons were emitted from hotter filaments (Fig. 3). The values were well reproduced in a single experiment, but discrepancies were significant between different experiments because the emission is controlled by many factors, including the impurities in and on the filament, the thermal and mechanical history of the filament, and the roughness of the filament surface. Coating the filament with an alkali earth element is known to enhance the electron emission, but the method of application greatly affects the emission efficiency, as noted by many previous workers (e.g. Chapters 7 and 8 of Van der Zeil [25]).

The incremental increase in the emission becomes smaller at higher temperatures and the emission reaches a plateau at a given setting (Fig. 3). Additional increases in the filament temperature have no effect on the emission. The emission apparently reaches the maximum value because of space-charge

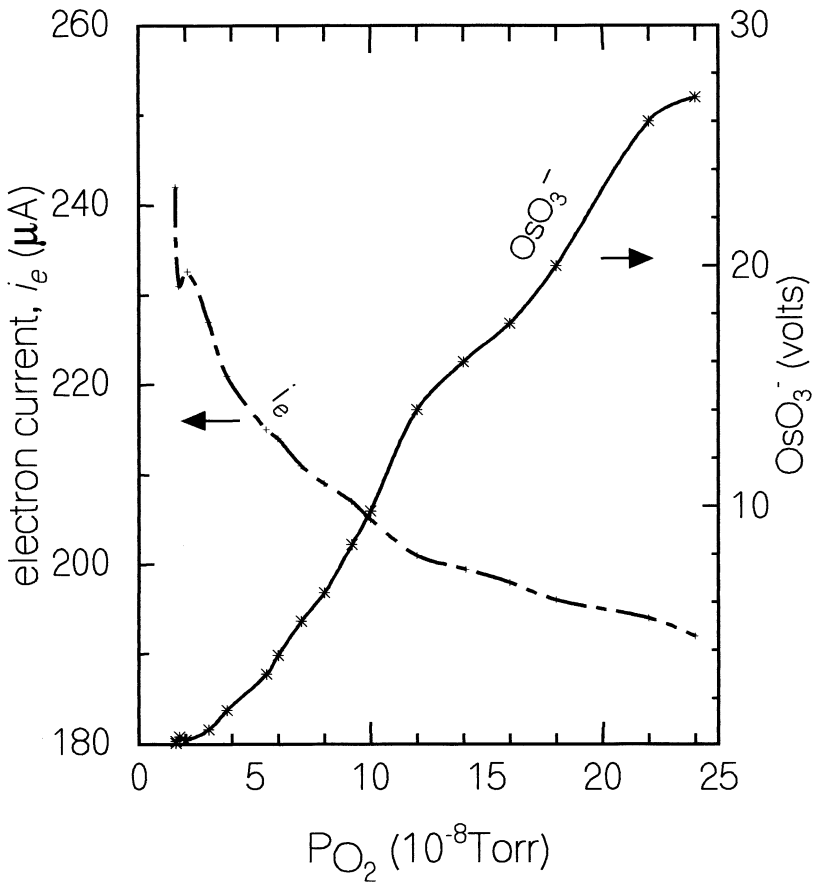

Fig. 4. Change in the thermal electrons and OsO_3^- with increasing P_{O_2}. P_{O_2} is the pressure measured between the ion pump and the source. Experimental condition: NBS-mounted Pt-filament, the filament current = 1.76 A.

limit. A high density of electrons, formed around the filament, repels electrons back to the filament.

3.2. Electron emission and OsO_3^-

At low temperatures, the intensity of OsO_3^- at the collector is positively correlated with total electron emissions (Fig. 3). At higher temperatures, the electron emission reaches space-charge limiting values, but the intensity of OsO_3^- increases with increasing filament current (Fig. 3). If the formation of OsO_3^- is primarily controlled by the electron emission, the intensity of OsO_3^- should also reach a plateau. Decoupling of the two shown in Fig. 3 indicates that thermal electrons do not limit the ionization of OsO_3^-. Instead, it is primarily controlled by the filament temperature.

The results suggest that the production of OsO_3^- can be achieved using other filament material and emitters. Other metals with lower electron emissions may be sufficient for the production of OsO_3^-. Barium salts have been used as an emitter (activator) by many researchers [3,21,24], but Ba, together with residual gases, produces molecules ($BaOBr^-$, BaOHBr, $BaCl_3$) that have persistent peaks in the mass range of OsO_3^- [21]. Other emitters, which have lower electron emission efficiency, may be used for the formation of OsO_3^-.

3.3. Electron emission versus O_2 pressure

The intensity of thermal electrons sharply decreases with increasing P_{O_2} at a given filament current

(Fig. 4). This is explained by increasing work function with increasing O_2 because electron emission (i_e) is expressed by

$$i_e \propto T^2 [\exp(-e\Phi)/kT]$$

where e = electronic charge, 1.6×10^{-19} C; Φ = electron work function; and k = Boltzmann constant, 1.38×10^{-23} J deg^{-1}. This is reproduced at different temperatures and different settings of extraction plates.

The decrease in electron emission at constant temperature in a given condition is explained by the "poisoning" effects of O_2 on the filament surface.

3.4. O_2 and OsO_3^-

A higher intensity of OsO_3^- is observed at higher P_{O_2} until 2×10^{-5} Torr at the ion pump ($1–2 \times 10^{-8}$ Torr without O_2, Fig. 4). This is consistent with earlier work [1,21,26], indicating that the formation of OsO_3^- is enhanced by O_2. An additional increase in O_2 results in decreasing OsO_3^-, as reported by many earlier workers [1,2,21]. Possible causes for the decline are (1) the formation of OsO_4^-, (2) collisions of OsO_3^- with O_2, (3) an uptake of electrons by O_2, and (4) the "poisoning" effect of O_2 on the filament, as described above. The formation of OsO_4^- will lower the amount of OsO_3^-, but we discount this as the significant cause because OsO_4^- peak intensities were always very small. Higher density of O_2 at higher P_{O_2} could lead to more collisions with OsO_3^- and its neutralization by an electron exchange. Second, excess O_2 can absorb thermal electrons, leaving fewer for ionization of Os oxides. Third, O_2 has "poisoning" effects on the electron emission, as mentioned above. Additionally, minor electronic currents running through the extraction plates by O^- may have minor effects on the source optics. These factors of (2), (3) and (4) are likely to contribute to decreasing peaks of OsO_3^- with increasing O_2.

4. Conversion of Os (O) to OsO_3^-

The formation of OsO_3^- from metal Os involves two steps: oxidation and negative ionization. Os in its native condition is very refractory, with a melting point of 3000°C, which makes its direct vaporization unlikely even under vacuum conditions. The volatilization through oxidation is promoted at higher temperatures, as shown by an exponential relationship between temperatures and OsO_3^- formation (Fig. 3). Os(VIII)O_4 is stable gas at room temperatures under atmospheric P_{O_2}, but very low OsO_4^-/OsO_3^- suggests that Os(VI)O_3 is predominant under low P_{O_2} ($<10^{-4}$ Torr) of the source.

4.1. Electron capture for ionization

Os oxides may be negatively charged by electrons or O^-. We believe that the former is the primary process because of the correlation between the total electron emission and OsO_3^- (Fig. 3). There is other supporting evidence. The electron density ($\sim 3 \times 10^{15}$ electrons/m^3) would be far greater than the concentration of O^- because the total O_2 is 3×10^{15} molecules/m^3 at 7.6×10^{-8} Torr. The concentration of negatively charged O^- should be far less than O_2; therefore, electrons are likely to be far more abundant than negatively charged O^-. This means that neutral OsO_3 molecules have higher probabilities of collision with electrons. A comparison of the total electron emission, $\sim 10^{-4}$ A and the ion current of OsO_3^- of 10^{-13} A, suggests that the electron abundance is far more than sufficient for the ionization of OsO_3.

Electrons move faster with increasing distance from the filament, which implies a higher density of electrons close to the filament. Since electron capture does not require high energy electrons, there is higher probability of ionization of OsO_3^- by electron capture close to the filament.

Electron capture is discounted as the ionization mechanism of Os oxides by Völkening et al. [2], on the basis of the temperature profile of OsO_3^-; the intensity of OsO_3^- increases with increasing temperatures, then decreases at higher temperatures. Because it was assumed by Völkening et al. ([2], p. 152) that electron emission increases at higher temperatures, the intensity of OsO_3^- should increase as the filament temperature increases. This was proposed as evidence against the electron capture hypothesis.

The evidence, however, is not necessarily in conflict with our proposed interpretation. More electrons will be collected by the extraction plates at higher temperatures, which will modify the voltage of the plates, and alter the source ion optics. Under these conditions OsO_3^- ions will no longer form a narrow focused beam.

4.2. Asymmetric tailed peaks of OsO_3^-

Without proper alignment of the source ion optics, the OsO_3^- ion beam commonly shows asymmetric peaks with sloped tops and tailing on the higher mass side [Fig. 5(a)], as noted by many researchers (e.g. Fig. 2 of Walcyzk et al. [1]) [21]. The asymmetric peaks indicate the formation of OsO_3^-, with a range of potential energies from ionization at different locations.

To examine further the cause for asymmetric peaks, we intentionally produced asymmetric peaks and collected the peaks in the narrowed collector slit [Fig. 5(b)]. The peaks have a gentler slope on the higher mass side because of the presence of excess OsO_3^-. The excess component, the measured intensity minus the symmetric component, forms a peak with the maximum at 0.1 u higher than the main peak [Fig. 5(c)]. This suggests at least two kinds of ionization.

The apparent mass difference (ΔM) is related to the potential difference (ΔV in V); $(1 + \Delta M/M) \propto 1/(1 + \Delta V/V)$. The mass difference of 0.1 u yields ~4 V in the potential energy difference. This is similar to the voltage where O_2 would be most efficiently ionized, ~3 V [27]. We, therefore, believe that the low energy OsO_3^- forming the second peak is probably related to the ionization by O^-. Neutral OsO_3 molecules collide with O^- away from the filament and subsequent electron exchange results in the ionization of the former:

$$OsO_3 + O^- = OsO_3^- + O^o$$

Alignment of the source optics can change the peak shape, and it is possible to produce peaks with long tails extending beyond the next peaks. This suggests that significant ionization can take place even farther away from the draw-out plates. Such low energy OsO_3^- ions are most likely formed through the interactions between charged and neutral species. Charged entities (e^-, O^-, and OsO_3^-) travel together because the deflection of charged particles in the electrostatic field is mass independent (p. 21 of Grivet [28]), and neutral molecules, O_2 and OsO_3, drift in the source. Collision between highly energetic charged species and neutral molecules of very low energy will lead to neutralization of the former and ionization of the latter. OsO_3 may drift away from the filaments and be ionized by electrons. Some OsO_3^- may be de-ionized by O_2 and ionized again by electrons or O^-. These OsO_3^- ions formed far from filament will have much lower potential energies than those formed on the filament and contribute to the long tailing of peaks.

Our proposed interpretation is supported by the change in the tail shape when a hand magnet is applied near the source, as reported by previous workers [7,18]. The measurements of electron currents through extraction plates showed sharp changes in the currents when a hand magnet was placed near the filament because the induced electromagnetic field strongly deflected lightweight electrons. Electrons probably spin tightly very near the filament, thus providing more opportunities for the ionization of Os near the filament and fewer opportunities far away from the filament.

5. Discussion

Thermal ionization mass spectrometry is commonly called surface ionization mass spectrometry, because ionization is considered to take place on the hot filament surface [15]. Ionization in N-TIMS is considered to be similar to that in P-TIMS, in that negative ions form at the filament surface [12,13,15,29] with small energy spread [14]. The results presented in this paper suggest that ionization in N-TIMS is more complicated and that not all ions form very close to the filaments. Our interpretation is consistent with commonly observed problems in N-

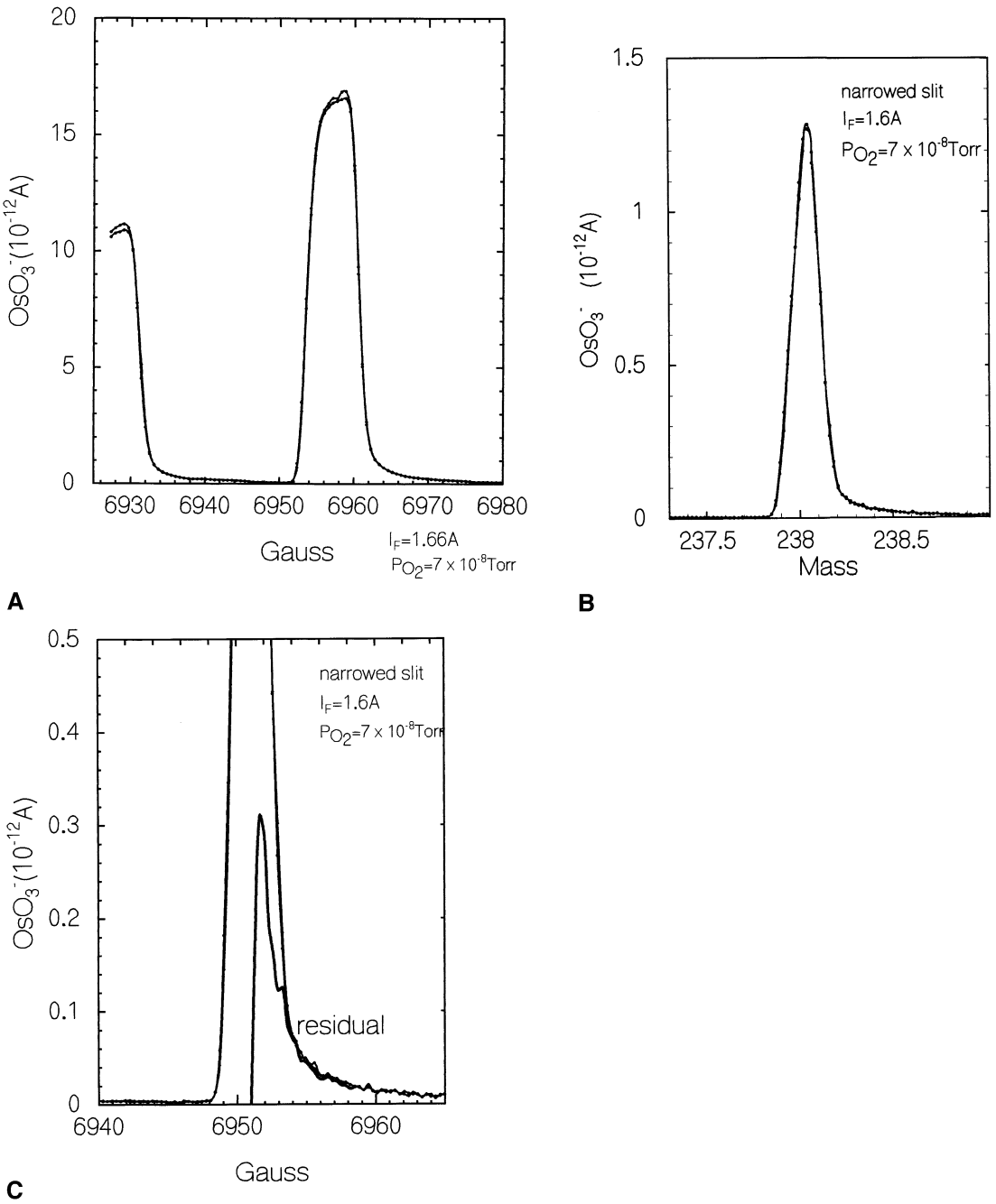

Fig. 5. (A) Scan of m/z 238 peak. Experimental condition: filament current = 1.6 A, $P_{O_2} = 7 \times 10^{-8}$ Torr. (B) Scan of the m/z 238 with a narrowed collector slit. (C) The peak scan by a narrowed collector slit. The small peak is an extra asymmetric component in the measured intensity, which is obtained by the measured intensity, subtracting the intensity predicted from the symmetry of the main peak. Experimental condition: filament current = 1.6 A, $P_{O_2} = 7 \times 10^{-8}$ Torr.

TIMS, such as "memory effects" during mass spectrometry.

5.1. Memory effects of mass spectrometry

It is well known among isotope geochemists that Re blank peaks are very high after running Re samples or after the use of Re filaments. This is also the reason why a single mass spectrometer cannot be used for Nd- and Pb-isotope analysis in the positive ion mode and for Os-isotope analysis in the negative ion mode because Nd- and Pb-isotope ratio measurements use Re filaments. In P-TIMS, ionization is restricted to the filament surface and only elements on or in the filament can be ionized and recorded in the collector.

In N-TIMS, ions far from the filament can be ionized because thermal electrons escape from the filament and are accelerated in the source. The electrons far from the filament may ionize elements and molecular species, which are not on or in the filament.

Re, W, and Ta are the most commonly used filament material for P-TIMS and they are sputtered onto the extraction plates and other internal surfaces of the source. Among them, Re may form volatile species by reacting with residual Cl in the mass spectrometer, Cl and O in the emitter (activator) on the filament, or O_2 gas introduced to the source. For example, chlorides, oxychloride, and oxides can easily be in a gaseous phase in the vacuum condition of the source because their melting points are relatively low (e.g. melting point of $ReCl_6$ = 29°C; of $ReOCl_4$ = 29.3°C, and of Re_2O_7 = 297°C). Thermal electrons during the mass spectrometric analysis of Os samples could easily ionize such gases.

Molybdenum is a common impurity in Re metal and Mo forms volatile chlorides and oxychloride. It is not surprising that MoO_3^- is reported to have interfered during N-TIMS of Ru isotopes [21].

Elements in samples and filaments sputter on extraction plates and the inner surface of the source and they may form volatile molecules during the subsequent sample analysis. These impure atoms and molecules may be ionized close to the filament and they would be recorded at their correct masses. Some, which are ionized far from the filament, may be misidentified as elements with higher mass numbers. Identification of "foreign" molecules and elements in N-TIMS may need extra caution. Extra care and cleanliness of extraction plates may be required for N-TIMS to minimize any contamination.

6. Comparison with P-TIMS

N-TIMS has been applied to the isotopic ratio measurements of B (BO_2^- [8,10,18]), O (PO_3^- [11]), Fe (FeF_4^- [30]), Tc (TcO_4^- [31]), Ru (RuO_3^- [6,21]), W (WO_3^- [5]), Re (ReO^- and ReO_2^- [32], ReO_3^- and ReO_4^- [3,15,23]). Ir (IrO_2^- [3,33]) and Pt (Pt^- [7], PtO_2^-, and PtO_3^- [34]). The isotopic ratio measurements require heat (filament temperature), thermal electrons, and O_2 in most cases but these components adversely influence ionization, which makes N-TIMS more complicated than P-TIMS. Here, we summarize the main differences between the two.

6.1. Distortion of electric field

In P-TIMS, the electric field of the source remains constant and the peak pattern is essentially identical during sample measurements because the positive ion current at the source plates is minuscule ($\leq 10^{-10}$ A) compared with the resistor chain current (1.77 mA). In N-TIMS, there is substantial electron flow from the filaments to the source plates (<100 μA). These currents can alter the plate potentials and change the preset optimum focusing conditions. The attendant distortion would allow low energy ions to pass through the exit slit, leading to erroneous isotopic ratio measurements.

In other cases, the distortion of the electric field at high temperatures could lead to the gradual decline and "disappearance" of peaks, as described above. It is also noted for RuO_3^- [6], IrO_2^- [4] and WO_3^- [16]. Völkening et al. [16] noted that the reduction of ion current "contradicts the theoretical approach" and that "the original intensity is reached" when "the filament temperature is reduced again." They attributed this "disagreement with the theoretical expectations" to

"nonequilibrium states, growing electron emission and shorter adsorption times of the species to be ionized." None of their explanations satisfactorily explains the reproducible ion current at a given filament temperature. Our proposed interpretation, distortion of the source ion optics by electrons, accounts for the behavior of ions.

Although O^- also contributes to the distortion to a very minor degree, the thermal electrons are the primary factor. The electron current at which the distortion starts depends on the element, the design of the source, and the accelerating voltage. We have observed the disappearance of OsO_3^- in other mass spectrometers and the effect is shown by Völkening et al. [2] and Walczyk et al. [1], but we have not observed it in our mass spectrometer using Pt filament at temperatures $\leq$1100°C.

6.2. Potential energies of ions: the effect on isotopic ratio measurements

In P-TIMS, vapor atoms are ionized on and very near an ionization filament. In a single filament assembly, the vaporization and ionization take place on one filament. The ionization is restricted to the surface or immediate vicinity of the filament, because thermal electrons are repelled back to the filaments by negatively charged extraction plates. This implies that ions have very similar potential energies, yielding well-defined symmetric peaks. Maximizing the peak height can optimize the source optics.

In N-TIMS, thermal electrons can be extracted by the electric field. The electrons escaping from the filament can ionize neutral molecules along their path, thus forming ions with low potential energies. The optimal source optics may not necessarily yield the highest peak intensities, because the negative ions have a range of potential energies. Maximizing the intensities of peaks allows lower energy ions to pass through the exit slit; thus, ions of the same mass are spread forming long tailing and possibly extending over different peaks at the collectors.

The high background and long tailings observed by previous workers during N-TIMS [6,7] are also attributed to the presence of ions with low potential energies. High and asymmetric background baselines lead to inaccurate base corrections for peaks. Hand magnets have been applied near the source to reduce the baseline [7], but the placement of hand magnets is not always easily controlled. The best remedy is to prevent low energy ions from entering the flight tube by proper focusing. Eliminating low energy ions lowers the peak height, but is essential for accurate isotopic ratio measurements.

Different isotopic ratios of *B* from a single sample have been observed at different filament temperatures and different sample size [10,18]. This too can be partly attributed to the presence of low energy ions. The filament temperature change is accompanied by the change in the electron emission and electron currents through extraction plates. This implies that realignment of the source optics and peak shape monitoring are essential for accurate isotope measurements whenever filament temperature is altered.

Acknowledgements

John Ludden and Chris Brooks of Université de Montréal donated the structural components of the mass spectrometer, "Olivia." Ron Doig of McGill University provided Cary components. The installation was supported by Natural Sciences and Engineering Research Council of Canada Equipment and Research grants to K.H., and benefitted from the expertise of the Science Technology Centre of Carleton University. We thank Gregory Ravizza of WHOI for his donation of the Os "shelf" solution. Comments by J. Blenkinsop of Carleton University, J. M. Edmond of MIT, John L. Holmes of the University of Ottawa, and Martin F. Miller and A. S. Cohen of the Open University are appreciated.

References

[1] T. Walczyk, E. H. Hebeda, K. G. Heumann, Fresenius J. Anal. Chem. 341 (1991) 537–541.

[2] J. Völkening, T. Walczyk, K. G. Heumann, Int. J. Mass Spectrom. Ion Processes 105 (1991) 147–159.
[3] R. A. Creaser, D. A. Papanastassiou, G. J. Wasserburg, Geochim. Cosmochim. Acta 55 (1991), 397–401.
[4] T. Walczyk, K. G. Heumann, Int. J. Mass Spectrom. Ion Processes 123 (1993) 139–147.
[5] C. L. Harper Jr., S. B. Jacobsen, Mineral Magazine 58A (1994) 378–379.
[6] M. Huang, Y. Liu, A. Masuda, Anal. Chem. 68 (1996) 841–844.
[7] C. S. J. Briche, P. D. P. Taylor, P. De Bièvre, Anal. Chem. 69 (1997) 791–793.
[8] N. L. Duchateau, P. De Bievrem J. Mass Spectrom. Ion Processes 54 (1983) 289–297.
[9] A. Vengosh, A. R. Chivas, M. T. McCulloch, Chem. Geol. 79 (1989) 333–343.
[10] U. S. Klötzli, Chem. Geol. 101 (1992) 111–122.
[11] C. Holmden, D. A. Papanastassion, G. J. Wasserburg, Geochim. Cosmochim. Acta 61 (1997) 2253–2263.
[12] H. Kawano, F. M. Page, Int. J. Mass Spectrom Ion Physics 50 (1983) 1–34.
[13] K. G. Heumann, S. Eisenhut, S. Gailus, E. H. Hebeda, R. Nusko, R. A. Vengosh, T. Walczyk, The Analyst 120 (1995) 1291–1299.
[14] D. Colodner, V. Salters, D. C. Duckworth, Anal. Chem. 66 (1994) 1079–1089.
[15] J. E. Delmore, J. Phys. Chem. 91 (1987) 2883–2886.
[16] J. Völkening, M. Köppe, K. Heumann, Int. J. Mass Spectrom. Ion Processes 107 (1991) 361–368.
[17] I. Lamgmuir, K. H. Kingdon, R. Soc. London Proc. 107 (1925) 61–79.
[18] N. G. Hemming, G. N. Hanson, Chem. Geol. 114 (1994) 147–156.
[19] K. G. Heumann, H. Zeininger, Int. J. Mass Spectrom. Ion Processes 67 (1985) 237–252.
[20] C. Moreno, Mass Sci. Technol. 7 (1996) 137–141.
[21] Q. Yin, N-TIMS Technique for the Re-Os and Ru Isotopic Systems and its Application to Selected Geochemical and Cosmochemical Problems, Ph.D. thesis, University of Mainz, 1995, p. 175.
[22] A. O. Nier, Phys. Rev. 77 (1950) 789–793.
[23] T. Walczyk, E. H. Hebeda, K. G. Heumann, Int. J. Mass Spectrom. Ion Processes 130 (1994) 237–246.
[24] E. H. Hauri, Geochemical and fluid dynamic investigations into the nature of chemical heterogeneity in the Earth's mantle. Ph.D. thesis, MIT-WHOI, 1992 239 p.
[25] A. Van der Ziel, Solid State Physical Electronics, 3rd ed., Prentice Hall, Englewood Cliffs, NJ, 1976 p. 528.
[26] E. Hauri, S. R. Hart, G. Ravizza, Proceedings of the Alfred O. Nier Symposium Inorganic Mass Spectrometry, 1991 p. 233.
[27] B. M. Smirnov, Negative Ions, McGraw-Hill, New York, 1982.
[28] P. Grivet, Electron Optics, Pergamon, New York, 1972.
[29] H. Zeininger, K. G. Heumann, Int. J. Mass Spectrom. Ion Phys. 48 (1983) 377–380.
[30] T. Walczyk, T. Int. J. Mass Spec. Ion Processes 161 (1997) 217–227.
[31] D. J. Rokop, N. C. Schroeder, K. Wolfsberg, Anal. Chem. 62 (1990) 1271–1274.
[32] N. R. Daly, R. G. Ridley, Nature 202 (1964) 896.
[33] A. D. Anbar, G. J. Wasserburg, D. A. Papanastassiou, P. S. Andersson, Science 273 (1996) 1524–1528.
[34] K. Hattori, D. P. Menagh, T. J. S. Cole, unpublished.
[35] A. O. Nier, Phys. Rev. 52 (1937) 885.